J. Fluid Mech. (2026), *vol.* 1037, R4, doi:10.1017/jfm.2026.11682



Taylor–Aris dispersion in shear-rate-dependent fluid flows

Evgeniy Boyko[1] **and Howard A. Stone**[2]

[1]Faculty of Mechanical Engineering, Technion – Israel Institute of Technology, Haifa 3200003, Israel
[2]Department of Mechanical and Aerospace Engineering, Princeton University, Princeton, NJ 08544, USA
Corresponding author: Evgeniy Boyko, evgboyko@technion.ac.il

(Received 3 February 2026 UTC; revised 31 March 2026 UTC; accepted 11 May 2026 UTC)

The spread of a pulse of solute in a pressure-driven channel flow is well described for a wide range of Newtonian flows for which the viscosity and diffusivity are constants. Over many decades, various extensions have been suggested for the dispersion in pressure-driven non-Newtonian channel flows. While many theoretical studies have examined the effect of shear-rate-dependent viscosity on dispersion for a variety of non-Newtonian constitutive models, the solute diffusivity has invariably been treated as a constant. This assumption, however, is in contrast to the expectation that the diffusivity of a colloidal particle is inversely related to the viscosity, e.g. recall the Stokes–Einstein relation. We account for this coupling of transport coefficients – viscosity and diffusivity – by assuming a generalised form of the Stokes–Einstein equation, inspired by the recognition that the viscosity is now a field, although only transport transverse to the main flow direction is relevant because of the common assumptions of Taylor–Aris dispersion. Thus, we derive a general formula for axial dispersion in steady, pressure-driven shear-rate-dependent flows in uniform channels. In particular, we apply our general relation to calculate the Taylor–Aris dispersion coefficient for steady flows of a shear-thinning Carreau fluid and a viscoelastic Phan-Thien–Tanner fluid. Finally, we highlight new theoretical questions raised by this transport situation, where the underlying diffusivity is also a (tensorial) field related to variations in viscosity.

Key words: dispersion, non-Newtonian flows, viscoelasticity

1. Introduction

The spreading of a localised bolus of chemical in a pipe or channel flow of a Newtonian fluid with constant viscosity μ_N involves the interplay of the velocity profile, with average

© The Author(s), 2026. Published by Cambridge University Press. This is an Open Access article, distributed under the terms of the Creative Commons Attribution licence (https://creativecommons.org/licenses/by/4.0/), which permits unrestricted re-use, distribution and reproduction, provided the original article is properly cited.

https://doi.org/10.1017/jfm.2026.11682 Published online by Cambridge University Press

speed $\langle u \rangle$, and the Brownian motion, or effective diffusion constant, D_N, of the solute. The spreading of solute is usually dominated by the flow as the velocity varies across a channel, thus acting to increase the distance between solute near the walls, in contrast to solute near the centre of the channel. In the case of laminar flows, Taylor (1953) and Aris (1956), following distinct approaches, described the long-time behaviour of a spreading solute in pressure-driven flow in uniform channels in terms of an effective (Taylor–Aris) axial dispersion coefficient, D_{eff}, that exceeds that of molecular diffusion by an amount proportional to $\langle u \rangle^2 a^2 / D_N$, where a is the pipe radius or channel height (Taylor 1953; Aris 1956). The enhanced spreading occurs because solute molecules can diffuse from fast streamlines to slow streamlines, and *vice versa*, with larger diffusion constants tending to make the solute distribution more uniform, thus reducing the dispersion coefficient.

Complex, non-Newtonian fluids can have a shear-rate-dependent viscosity, which changes the velocity profile, even in simple geometries such as pressure-driven pipe or channel flow. For example, common inelastic constitutive equations relating the strain rate to the stress, such as power-law, Ellis, Carreau and Casson models, as well as viscoelastic descriptions, such as Phan-Thien–Tanner, Giesekus and a finitely extensible nonlinear elastic (FENE) model with the Peterlin approximation (FENE-P), all display a shear-rate-dependent viscosity (Bird, Armstrong & Hassager 1987). Because the velocity profile changes across the channel, a change in the dispersion coefficient is expected. We note that for the Oldroyd-B and FENE-CR models, there is no shear thinning and no change in the velocity profile from that of a Newtonian fluid for fully developed pressure-driven flow in a straight channel (see, e.g. Mahapatra *et al.* 2025).

There are many studies in the literature, spanning at least the past six decades, that describe the flow-enhanced contribution to solute dispersion in complex fluids (Fan & Hwang 1965; Booras & Krantz 1976; Sharp 1993; Dash, Jayaraman & Mehta 2000; Nagarani & Sebastian 2013; Rana & Murthy 2016*a*,*b*; Singh & Murthy 2023; Teodoro, Bautista & Méndez 2025). Nevertheless, the corresponding dispersion coefficient of a colloidal solute also depends on the background particle diffusivity, which itself should be expected to depend on the local viscosity, in which case it would also depend on the shear rate; i.e. the diffusion coefficient that forms the basis for sampling the velocity distribution changes from D_N. In particular, for a constant viscosity Newtonian solvent (μ_N) and a solute with effective radius b, the Stokes–Einstein relation is $D_N = k_B T/(6\pi b \mu_N)$, where k_B is the Boltzmann constant and T is the temperature. Denoting the local shear rate as $\dot{\gamma}$, then, since we consider a shear-rate-dependent viscosity, $\mu(\dot{\gamma})$, we expect for particles large compared with the typical polymer length scales (see § 2.3) the corresponding diffusion coefficient D to be inversely related to $\mu(\dot{\gamma})$, consistent with theoretical considerations of particle diffusion in polymer solutions and melts (Brochard-Wyart & de Gennes 2000; Cai, Panyukov & Rubinstein 2011); $D \neq D_N$. Therefore, in our analysis we assume a generalised form of the Stokes–Einstein relation for the local diffusivity $D(\dot{\gamma}) = D_0 \mu_0 / \mu(\dot{\gamma})$, where we denote the zero-shear-rate viscosity of the fluid as μ_0 with corresponding diffusivity D_0. We note, as discussed more below, that although the viscosity is now a field, i.e. it varies with position, because of the common assumptions of Taylor–Aris dispersion, only transport transverse to the main flow direction (a scalar field) is relevant here.

To the best of our knowledge, the fact that the diffusivity may vary spatially, due to the shear-rate-dependent viscosity, has not been recognised in most, if not all, of the theoretical literature on Taylor–Aris dispersion in complex fluids. In particular, a shear-rate-dependent viscosity not only affects the velocity profile that sets the axial rate of spreading, which is treated in the large existing literature, but it also influences the transverse diffusion that

https://doi.org/10.1017/jfm.2026.11682 Published online by Cambridge University Press

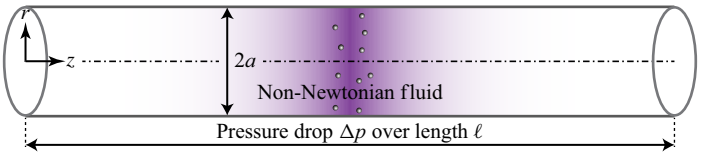


Figure 1. Schematic illustration of the examined configuration for Taylor–Aris dispersion of a complex fluid. The imposed pressure drop Δp drives the steady flow of a non-Newtonian fluid through an axisymmetric channel of length ℓ and radius a. Our interest lies in elucidating the impact of shear-rate-dependent diffusivity on the dispersion of passive tracers in a non-Newtonian flow.

sets the rate of sampling different streamlines, which has not been taken into account in previous studies of Taylor–Aris dispersion in complex fluid flows.

In this work, using the approximate Stokes–Einstein model described above (but see § 2.3), we provide a systematic derivation of the Taylor–Aris dispersion in pressure-driven shear-rate-dependent flows in uniform channels, and find

$$\frac{D_{eff}}{D_0} = \mathcal{A} + \mathcal{B}Pe^2, \tag{1.1}$$

where $\mathcal{A}$ and $\mathcal{B}$ are the non-dimensional functions that depend on the shear-rate-dependent fluid rheology, and Pe is the Péclet number, $Pe = \Delta p a^3/(8D_0\mu_0\ell)$, for a steady flow driven by a pressure difference Δp over a length scale ℓ. In all previous studies, the first coefficient is $\mathcal{A} = 1$, while the second coefficient $\mathcal{B}$ incorporates certain rheological effects but has not recognised a change in the diffusion coefficient with shear rate. In contrast, we account for the dependence of the diffusion coefficient on the local shear rate through shear-rate-dependent viscosity. As a result, our predictions for both $\mathcal{A}$ and $\mathcal{B}$ differ from the results available in the literature. In § 2, we present the theoretical framework for calculating the effective dispersion coefficient of the shear-rate-dependent fluid flow through an axisymmetric channel, deriving (1.1) and highlighting the shear-rate dependence of the coefficients $\mathcal{A}$ and $\mathcal{B}$. We also briefly discuss in § 2.3 research questions raised by this kind of Brownian transport question, where the viscosity is a field. In § 3, we illustrate the use of our main result, (1.1), and calculate the effective shear-rate-dependent dispersion coefficient for steady flows of a shear-thinning Carreau fluid and a viscoelastic Phan-Thien–Tanner fluid. We conclude with a discussion of the results in § 4.

2. Analysis of Taylor–Aris dispersion in shear-rate-dependent fluid flows

We study the role of a shear-rate-dependent viscosity on the dispersion of passive tracers when placed in a steady pressure-driven flow of a non-Newtonian fluid in an axisymmetric channel of radius a and length ℓ. We assume that the imposed pressure drop Δp drives the incompressible steady flow and induces the fluid motion with pressure distribution p and velocity $\boldsymbol{u}$. Given the azimuthal symmetry, we employ an axisymmetric cylindrical coordinate system (r, z) to describe the flow, as shown in figure 1.

2.1. *Derivation of the one-dimensional, cross-sectionally averaged advection–diffusion equation*

Here, we begin with the (three-dimensional) advection–diffusion equation, and through an averaging approach, we arrive at a one-dimensional Taylor–Aris description for axial dispersion. Although a shear-rate-dependent viscosity means that the properties of the fluid may vary non-isotropically, we simply use D as a scalar field of the shear rate. Under the assumptions of the azimuthal symmetry and a unidirectional flow in the axial

https://doi.org/10.1017/jfm.2026.11682 Published online by Cambridge University Press

direction, $\boldsymbol{u} = u(r)\boldsymbol{e}_z$, while neglecting the feedback of concentration on the velocity field, the concentration of passive tracers $c(r, z, t)$ evolves according to the advection–diffusion equation

$$\frac{\partial c}{\partial t} + u\frac{\partial c}{\partial z} = \frac{1}{r}\frac{\partial}{\partial r}\left(rD(\dot{\gamma})\frac{\partial c}{\partial r}\right) + \frac{\partial}{\partial z}\left(D(\dot{\gamma})\frac{\partial c}{\partial z}\right), \tag{2.1}$$

where $D(\dot{\gamma})$ is the diffusion coefficient of the solute particle that depends on the local shear rate $\dot{\gamma} = |\mathrm{d}u(r)/\mathrm{d}r|$. The governing equation (2.1) is supplemented by the no-flux boundary condition at the channel walls, $\partial c/\partial r = 0$ at $r = a$.

For the Taylor–Aris analysis, we follow the notation of Stone & Brenner (1999) (see also Taylor (1953)) and expand each variable into cross-sectional averages of the form

$$\langle(\cdot)\rangle = \frac{1}{\pi a^2}\int_0^a (\cdot)2\pi r\mathrm{d}r = \frac{2}{a^2}\int_0^a (\cdot)r\mathrm{d}r, \tag{2.2}$$

and deviations from cross-sectionally averaged quantities defined by writing

$$c(r, z, t) = \langle c\rangle\,(z, t) + c'(r, z, t) \quad \text{and} \quad u(r) = \langle u\rangle + u'(r). \tag{2.3}$$

Substituting (2.3) into (2.1) yields

$$\frac{\partial\,\langle c\rangle}{\partial t} + \frac{\partial c'}{\partial t} + \langle u\rangle\,\frac{\partial\,\langle c\rangle}{\partial z} + u'\frac{\partial\,\langle c\rangle}{\partial z} + \langle u\rangle\,\frac{\partial c'}{\partial z} + u'\frac{\partial c'}{\partial z} = \frac{1}{r}\frac{\partial}{\partial r}\left(rD\frac{\partial c'}{\partial r}\right) + D\frac{\partial^2\,\langle c\rangle}{\partial z^2} + D\frac{\partial^2 c'}{\partial z^2}, \tag{2.4}$$

where $D(\dot{\gamma})$ solely depends on the radial coordinate.

Noting that $\langle\langle c\rangle\rangle = \langle c\rangle$ and $\langle c'\rangle = \langle u'\rangle = 0$, we can average (2.4) over the channel cross-section, use the no-flux boundary condition, which, upon averaging, then eliminates the first term after the equal sign, and recognise that $\langle D(\partial^2\langle c\rangle/\partial z^2)\rangle = \langle D\rangle(\partial^2\langle c\rangle/\partial z^2)$, which allows us to obtain

$$\frac{\partial\,\langle c\rangle}{\partial t} + \langle u\rangle\,\frac{\partial\,\langle c\rangle}{\partial z} + \left\langle u'\frac{\partial c'}{\partial z}\right\rangle = \langle D\rangle\,\frac{\partial^2\,\langle c\rangle}{\partial z^2} + \left\langle D\frac{\partial^2 c'}{\partial z^2}\right\rangle. \tag{2.5}$$

Next, subtracting (2.5) from (2.4), we obtain

$$\begin{aligned}\frac{\partial c'}{\partial t} + u'\frac{\partial\,\langle c\rangle}{\partial z} + \langle u\rangle\,\frac{\partial c'}{\partial z} + u'\frac{\partial c'}{\partial z} - \left\langle u'\frac{\partial c'}{\partial z}\right\rangle \\ = \frac{1}{r}\frac{\partial}{\partial r}\left(rD\frac{\partial c'}{\partial r}\right) + (D - \langle D\rangle)\,\frac{\partial^2\,\langle c\rangle}{\partial z^2} + D\frac{\partial^2 c'}{\partial z^2} - \left\langle D\frac{\partial^2 c'}{\partial z^2}\right\rangle.\end{aligned} \tag{2.6}$$

Consistent with a Taylor–Aris dispersion analysis, we are interested in the long-time behaviour of cross-stream diffusion, that is, axial distances $\ell \gg \langle u\rangle a^2/D$, and we consider that $|c'|/\langle c\rangle \ll 1$ so that variations of the concentration across the channel are small. Under these assumptions, from an order-of-magnitude analysis, it follows that (2.5) and (2.6) simplify to (see, e.g. Griffiths & Stone 2012)

$$\frac{\partial\,\langle c\rangle}{\partial t} + \langle u\rangle\,\frac{\partial\,\langle c\rangle}{\partial z} \approx \langle D\rangle\,\frac{\partial^2\,\langle c\rangle}{\partial z^2} - \left\langle u'\frac{\partial c'}{\partial z}\right\rangle, \tag{2.7}$$

and

$$u'\frac{\partial\,\langle c\rangle}{\partial z} \approx \frac{1}{r}\frac{\partial}{\partial r}\left(rD(\dot{\gamma})\frac{\partial c'}{\partial r}\right). \tag{2.8}$$

https://doi.org/10.1017/jfm.2026.11682 Published online by Cambridge University Press

The next key step in our analysis is the use of a generalised form of the Stokes–Einstein relation

$$D(\dot{\gamma}) = \frac{k_B T}{6\pi b \mu(\dot{\gamma})\chi} = \frac{D_0 \mu_0}{\mu(\dot{\gamma})} = \frac{D_0}{\mathcal{M}(\dot{\gamma})} \quad \text{with} \quad D_0 = \frac{k_B T}{6\pi b \mu_0 \chi} \text{ and } \mathcal{M} = \frac{\mu(\dot{\gamma})}{\mu_0}, \tag{2.9}$$

where $\mu(\dot{\gamma})$ is the shear-rate-dependent viscosity of the fluid evaluated at the location of the centre of the particle and μ_0 is the zero-shear-rate viscosity, so that the zero-shear-rate diffusivity D_0 is $D_0 = k_B T/(6\pi b \mu_0 \chi)$. Note that we have introduced a constant factor χ as an approximate model to account for the fact that the microscopic problem at the scale of a diffusing object now involves a viscosity field, i.e. the viscosity is a function of position. For the constant viscosity Newtonian limit, $\mu_0 = \mu_N$, we have $\chi = 1$ and $D_0 = D_N$. For convenience, we have also defined the dimensionless shear-rate-dependent viscosity $\mathcal{M} = \mu(\dot{\gamma})/\mu_0$, which is central to the calculation below.

Substituting (2.9) into (2.7) and (2.8), we obtain

$$\frac{\partial \langle c \rangle}{\partial t} + \langle u \rangle \frac{\partial \langle c \rangle}{\partial z} \approx D_0 \left\langle \mathcal{M}^{-1} \right\rangle \frac{\partial^2 \langle c \rangle}{\partial z^2} - \left\langle u' \frac{\partial c'}{\partial z} \right\rangle, \tag{2.10}$$

and

$$u' \frac{\partial \langle c \rangle}{\partial z} \approx \frac{D_0}{r} \frac{\partial}{\partial r} \left(r \mathcal{M}^{-1}(\dot{\gamma}) \frac{\partial c'}{\partial r} \right). \tag{2.11}$$

We remind the reader that, similar to $D(\dot{\gamma})$, the viscosity $\mathcal{M}(\dot{\gamma})$ solely depends on the radial coordinate r. Integrating (2.11) once with respect to r, while demanding that $c'(r, z, t)$ is finite at $r = 0$, yields

$$\frac{\partial c'(r, z, t)}{\partial r} = \frac{1}{D_0} \frac{\partial \langle c \rangle (z, t)}{\partial z} \frac{\mathrm{d} f(r)}{\mathrm{d} r} \quad \text{with} \quad \frac{\mathrm{d} f(r)}{\mathrm{d} r} = \frac{\mathcal{M}(\dot{\gamma})}{r} \int_0^r u'(r') r' \mathrm{d} r'. \tag{2.12}$$

Integrating (2.12) with respect to r, we obtain

$$c'(r, z, t) = c'(0, z, t) + \frac{1}{D_0} \frac{\partial \langle c \rangle (z, t)}{\partial z} [f(r) - f(0)], \tag{2.13a}$$

with

$$f(r) - f(0) = \int_0^r \frac{\mathcal{M}(\dot{\gamma}(r'))}{r'} \int_0^{r'} u'(s) s \mathrm{d} s \mathrm{d} r', \tag{2.13b}$$

where $c'(0, z, t)$ can be determined from the requirement that $\int_0^a c' r \mathrm{d} r = 0$, consistent with the definition $\langle c' \rangle = 0$.

We aim to calculate the final term on the right-hand side of (2.10), which represents the dispersion produced by the coupling of molecular diffusion and the variation of velocity in the cross-section. To this end, we substitute (2.13) into the last term of the right-hand side of (2.10) to obtain

$$\left\langle u' \frac{\partial c'}{\partial z} \right\rangle = \frac{2}{a^2 D_0} \int_0^a \left\{ u'(r) r \int_0^r \left[\frac{\mathcal{M}(\dot{\gamma}(r'))}{r'} \left(\int_0^{r'} u'(s) s \mathrm{d} s \right) \right] \mathrm{d} r' \right\} \mathrm{d} r \frac{\partial^2 \langle c \rangle}{\partial z^2}, \tag{2.14}$$

where we have used the fact that $\langle u' \partial c'(0, z, t)/\partial z \rangle = 0$.

Integrating by parts and noting that $\langle u' \rangle = \int_0^a u'(r) r \mathrm{d} r = 0$, (2.14) can be expressed as

$$\left\langle u' \frac{\partial c'}{\partial z} \right\rangle = -\frac{2}{a^2 D_0} \int_0^a \frac{\mathcal{M}(\dot{\gamma}(r))}{r} \left(\int_0^r u'(r') r' \mathrm{d} r' \right)^2 \mathrm{d} r \frac{\partial^2 \langle c \rangle}{\partial z^2}. \tag{2.15}$$

https://doi.org/10.1017/jfm.2026.11682 Published online by Cambridge University Press

Finally, substituting (2.15) into (2.10) and using (2.2), we obtain the following advection–diffusion equation for the evolution of the area-averaged concentration:

$$\frac{\partial \langle c\rangle}{\partial t} + \langle u\rangle \frac{\partial \langle c\rangle}{\partial z} \approx D_{eff}\frac{\partial^2 \langle c\rangle}{\partial z^2}, \tag{2.16}$$

where D_{eff} is the effective shear-rate-dependent dispersion coefficient, given as

$$D_{eff} = \frac{2D_0}{a^2}\left[\int_0^a \frac{r}{\mathcal{M}(r)}\mathrm{d}r + \frac{1}{D_0^2}\int_0^a \frac{\mathcal{M}(r)}{r}\left(\int_0^r u'(r')r'\mathrm{d}r'\right)^2 \mathrm{d}r\right], \tag{2.17}$$

which has the structure of a traditional Taylor–Aris dispersion analysis.

Scaling by the characteristic dimensions, we introduce the following non-dimensional variables $\tilde{r} = r/a$, $\tilde{u} = u/u_c$, $\tilde{u}' = u'/u_c$ and $\mathcal{M} = \mu/\mu_0$, where $u_c = \Delta p a^2/(8\mu_0\ell)$ is the characteristic velocity scale. With this non-dimensionalisation, (2.17) can be expressed in a non-dimensional form as

$$\frac{D_{eff}}{D_0} = \underbrace{2\int_0^1 \frac{\tilde{r}}{\mathcal{M}(\tilde{r})}\mathrm{d}\tilde{r}}_{\mathcal{A}} + \underbrace{2\int_0^1 \frac{\mathcal{M}(\tilde{r})}{\tilde{r}}\left(\int_0^{\tilde{r}} \tilde{u}'(\tilde{r}')\tilde{r}'\mathrm{d}\tilde{r}'\right)^2 \mathrm{d}\tilde{r}}_{\mathcal{B}} Pe^2 = \mathcal{A} + \mathcal{B}Pe^2, \tag{2.18}$$

where $Pe = u_c a/D_0 = \Delta p a^3/(8D_0\mu_0\ell)$ is the Péclet number, and $\mathcal{A}$ and $\mathcal{B}$ are the non-dimensional coefficients that depend on the fluid rheology.

Equation (2.18) is the main result of this study and highlights several features: (i) in the absence of non-Newtonian effects, the dispersion coefficient results in the classical Pe^2 scaling, i.e. it varies with the square of the average speed or shear rate. (ii) For a non-Newtonian fluid, when the diffusion coefficient D is independent of shear rate, such that $\mathcal{M} \equiv 1$ in (2.18), there is a rheological contribution from the integral involving the velocity profile, which has been accounted for in previous studies (see, e.g. Fan & Hwang 1965; Booras & Krantz 1976; Sharp 1993; Teodoro *et al.* 2025). (iii) However, the dependence of viscosity and corresponding diffusivity on shear rate clearly indicates that the coefficients $\mathcal{A}$ and $\mathcal{B}$ are influenced by the fluid rheology through the viscosity and velocity profiles. In particular, the coefficient $\mathcal{A}$ depends on the viscosity distribution, differing from the value of 1 found in previous studies on Taylor–Aris dispersion analysis in non-Newtonian fluids. Furthermore, the coefficient $\mathcal{B}$ depends on both the viscosity distribution and the deviation from the cross-sectionally averaged velocity profile, in contrast to previous studies that accounted only for the velocity and not for the variation in diffusivity through the viscosity distribution (see, e.g. Sharp 1993; Teodoro *et al.* 2025).

We note that for pressure-driven flow of a Newtonian fluid with a constant viscosity $\mu_0 = \mu_N$ ($\mathcal{M} = 1$), we have $\tilde{u}(\tilde{r}) = 2(1-\tilde{r}^2)$ and $\tilde{u}'(\tilde{r}) = 1 - 2\tilde{r}^2$. Using (2.18), we find that $D_{eff}/D_0 = 1 + Pe^2/48$, as originally found by Taylor (1953).

2.2. *The cross-sectionally averaged concentration distribution*

The cross-sectionally averaged concentration distribution follows from the solution of (2.16), which is a standard advection–diffusion equation with constant coefficients $\langle u\rangle$ and D_{eff}. Nevertheless, we note that, for pressure-driven flow of a non-Newtonian fluid, both $\langle u\rangle$ and D_{eff} change depending on the constitutive description. For example, for a given number of passive tracers, $N_0 = \pi a^2 \int_{-\infty}^{\infty}\langle c\rangle(z,t)\mathrm{d}z$, injected at time $t = 0$ into the

https://doi.org/10.1017/jfm.2026.11682 Published online by Cambridge University Press

flow at $z = z_0$, the well-known analytical solution of (2.16) takes the form (Taylor 1953)

$$\langle c\rangle(z,\, t) = \frac{N_0}{\pi a^2}\frac{1}{\sqrt{4\pi D_{eff} t}}\exp\left[-\frac{(z-(z_0+\langle u\rangle t))^2}{4D_{eff} t}\right], \tag{2.19}$$

representing a Gaussian distribution centred at $z_0 + \langle u\rangle t$.

For a Newtonian fluid, $\langle u\rangle = \Delta p a^2/(8\mu_N \ell)$ and $D_{eff}/D_N = 1 + Pe^2/48$. However, for non-Newtonian flows with shear-rate-dependent viscosity, both the average velocity $\langle u\rangle$ and the effective dispersion coefficient $D_{eff}/D_0 = \mathcal{A} + \mathcal{B}Pe^2$ change depending on the constitutive description due to the fluid rheology.

2.3. *Remark on a generalised form of the Stokes–Einstein relation*

It is well known that, for Newtonian fluids, the diffusivity of a Brownian particle is inversely proportional to the viscosity, as described by the classical Stokes–Einstein relation. However, no such understanding exists for the diffusivity of a particle in non-Newtonian fluid flow with shear-rate-dependent viscosity. Even for the case of diffusion of a colloidal particle of radius b in a polymer solution at rest, the dynamics depends on several length scales, e.g. the monomer or Kuhn length ℓ_K, a correlation length ℓ_{cor}, a measure of the entanglement length ℓ_{ent} and the radius of gyration of a polymer ℓ_{rg}. Typically, we expect $\ell_K < \ell_{cor}$, $\ell_{ent} < \ell_{rg}$. Theory (Brochard-Wyart & de Gennes 2000; Cai *et al.* 2011) and experiments (Kohli & Mukhopadhyay 2012; Nath *et al.* 2018; Chen *et al.* 2018) show that, for a complex fluid at rest, a Stokes–Einstein-like description of the particle diffusion coefficient is reasonable for $b > \ell_{rg}$, i.e. the diffusion coefficient is expected to be inversely related to the zero-shear-rate viscosity. We note that for small enough solutes the diffusion coefficient is similar, but not equal, to that in the solvent (Cai *et al.* 2011), in which case we expect the results in the literature with $D = \text{const.}$ to hold. These remarks support, at least for some systems, the approximate axial dispersion model offered in this work.

We are not aware of theoretical or experimental studies on how the diffusion coefficient of a colloidal particle varies with shear rate in non-Newtonian flows. Therefore, it is our understanding that the form of the relation between the diffusivity and the shear-rate-dependent viscosity, even in steady non-Newtonian fluid flows, remains an open research question.

As we understand the transport question at the scale of a colloidal (diffusing) particle, for flows as studied in this work, where there are steady viscosity variations, the necessary next steps would be to solve for the analogue of the Stokes–Einstein equation involving the hydrodynamic mobility of the diffusing particle. Some research that has hydrodynamic features of this kind of viscosity-gradient problem has been considered in recent years in the colloid science (Rings *et al.* 2010; Oppenheimer, Navardi & Stone 2016), microrheology (Squires & Mason 2010; Furst & Squires 2017) and active matter communities (Malgaretti, Popescu & Dietrich 2016; Liebchen *et al.* 2018; Datt & Elfring 2019; Esparza López *et al.* 2021).

3. Illustration of results

To illustrate the use of our main result (2.18), in this section, we calculate the effective shear-rate-dependent dispersion coefficient for a shear-thinning fluid described by the Carreau model and a viscoelastic fluid described by the simplified Phan-Thien–Tanner model.

https://doi.org/10.1017/jfm.2026.11682 Published online by Cambridge University Press

For a fully developed unidirectional flow in a straight axisymmetric channel, the axial Cauchy momentum equation simplifies to

$$\frac{\mathrm{d}p}{\mathrm{d}z} = -\frac{\Delta p}{\ell} = \frac{1}{r}\frac{\mathrm{d}(r\tau_{rz})}{\mathrm{d}r}, \tag{3.1}$$

where, for a straight channel, the pressure gradient is constant and can be expressed as $\mathrm{d}p/\mathrm{d}z = -\Delta p/\ell$. The shear stress component τ_{rz} of the deviatoric stress tensor $\boldsymbol{\tau}$ entails the description of the non-Newtonian fluid rheology and necessitates the use of a specific constitutive equation for $\boldsymbol{\tau}$ (and τ_{rz}). For a given constitutive description, one can find the viscosity $\mathcal{M}(\tilde{r})$ and the velocity $\tilde{u}(\tilde{r})$ required for calculating the dispersion coefficient.

3.1. *Shear thinning: Carreau model*

To account for the shear-thinning rheology of the fluid, we consider the Carreau viscosity model for $\mu(\dot{\gamma})$, which describes three experimentally observed behaviours of viscosity, namely, plateaus in viscosity at very low or very high shear rates and power-law dependence at intermediate shear rates. The constitutive equation for a Carreau viscosity model is (Carreau 1972; Bird *et al.* 1987)

$$\mu(\dot{\gamma}) = \mu_\infty + (\mu_0 - \mu_\infty)\left(1 + (\lambda_C\dot{\gamma})^2\right)^{(n-1)/2}, \tag{3.2}$$

where μ_0 and μ_∞ are the zero- and infinite-shear-rate viscosities, respectively. The power-law index n characterises the degree of shear thinning ($0 < n \leq 1$) and λ_C is the inverse of a characteristic shear rate at which shear thinning becomes apparent. The case $n = 1$, $\lambda_C = 0$, or $\mu_0 = \mu_\infty$ represents the Newtonian fluid with a constant viscosity μ_0.

Using the generalised Newtonian model, $\boldsymbol{\tau} = \mu(\dot{\gamma})(\boldsymbol{\nabla u} + (\boldsymbol{\nabla u})^{\mathrm{T}})$, the axial momentum equation (3.1) takes the form

$$-\frac{\Delta p}{\ell} = \frac{1}{r}\frac{\mathrm{d}}{\mathrm{d}r}\left(r\mu(\dot{\gamma})\frac{\mathrm{d}u}{\mathrm{d}r}\right) \quad \text{with} \quad \dot{\gamma} = -\frac{\mathrm{d}u}{\mathrm{d}r}. \tag{3.3}$$

Integrating (3.3) with respect to r and using the regularity of solution at $r = 0$, we obtain

$$-\frac{\Delta p}{\ell}\frac{r}{2} = \mu(\dot{\gamma})\frac{\mathrm{d}u}{\mathrm{d}r}, \tag{3.4}$$

so that the shear rate is $\dot{\gamma} = r\Delta p/(2\mu(\dot{\gamma})\ell)$. Substituting the latter result into the constitutive equation for the viscosity function results in an implicit nonlinear algebraic equation for μ, which for the Carreau model (3.2) takes the dimensionless form

$$\mathcal{M} = \beta + (1-\beta)\left(1 + \left(Cu\tilde{r}\mathcal{M}^{-1}\right)^2\right)^{(n-1)/2}, \tag{3.5}$$

where $\beta = \mu_\infty/\mu_0$, $\tilde{r} = r/a$ and $Cu = \lambda_C\Delta p a/2\mu_0\ell$ is the Carreau number based on the pressure drop Δp (Boyko & Stone 2021; Zhong *et al.* 2022). For given values of Cu, n, β, we solve numerically (3.5) using MATLAB's routine `fzero` to obtain the viscosity distribution $\mathcal{M}(\tilde{r})$.

Knowing the viscosity distribution $\mu(r)$ (or $\mathcal{M}(\tilde{r})$), we can integrate (3.4) again with respect to r and apply the no-slip boundary conditions on the channel walls to obtain the dimensional and corresponding non-dimensional axial velocity

$$u(r) = \frac{\Delta p}{2\ell}\int_r^a \frac{r'}{\mu(r')}\mathrm{d}r', \qquad \tilde{u}(\tilde{r}) = 4\int_{\tilde{r}}^1 \frac{\tilde{r}'}{\mathcal{M}(\tilde{r}')}\mathrm{d}\tilde{r}', \tag{3.6}$$

https://doi.org/10.1017/jfm.2026.11682 Published online by Cambridge University Press

	Low-Cu asymptote	Power-law asymptote	High-Cu asymptote
$\mathcal{M}(\tilde{r})$	1	$(Cu\tilde{r})^{(n-1)/n}$	β
$\tilde{u}(\tilde{r})$	$2(1-\tilde{r}^2)$	$\frac{4n}{n+1}Cu^{(1-n)/n}(1-\tilde{r}^{(n+1)/n})$	$(2/\beta)(1-\tilde{r}^2)$
$\mathcal{A}$	1	$\frac{2n}{n+1}Cu^{(1-n)/n}$	$1/\beta$
$\mathcal{B}$	1/48	$\frac{32n^4}{3(3n+1)^2(35n^2-2n-1)}Cu^{(1-n)/n}$	$1/(48\beta)$

Table 1. A summary of the low-Cu, power-law and high-Cu asymptotic expressions for $\mathcal{M}(\tilde{r})$ and $\tilde{u}(\tilde{r})$, as well as $\mathcal{A}$ and $\mathcal{B}$ appearing in the effective shear-rate-dependent dispersion coefficient (2.18), for the case of a shear-thinning Carreau fluid in an axisymmetric channel. For a description of this flow, see Zhong *et al.* (2022).

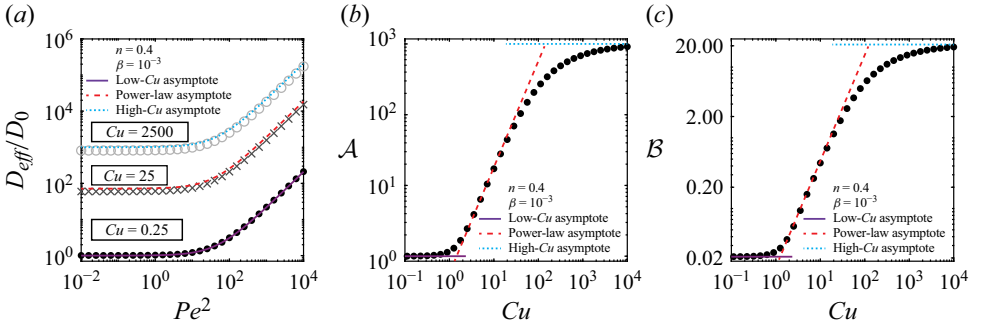


Figure 2. The effective shear-rate-dependent dispersion coefficient for a shear-thinning Carreau fluid in an axisymmetric channel. (*a*) Theoretically predicted value of D_{eff}/D_0 as a function of the square of the Péclet number, Pe^2, for different values of the Carreau number Cu. Coefficients (*b*) $\mathcal{A}$ and (*c*) $\mathcal{B}$, defined in (2.18), versus $Cu = \lambda_C \Delta p a/2\mu_0 \ell$. Dots, crosses and circles represent the semi-analytical results obtained by solving numerically (2.18) using (3.5) and (3.6). Purple solid and cyan dotted lines represent the asymptotic solutions for $Cu \ll 1$ and $Cu \gg 1$, respectively. Red dashed lines represent the power-law asymptotic solution for intermediate values of Cu. The asymptotic solutions are summarised in table 1. All calculations were performed using $n = 0.4$ and $\beta = \mu_\infty/\mu_0 = 10^{-3}$.

so that $\tilde{u}'(\tilde{r})$ is calculated from (3.6). We present in figure 2(*a*) the dimensionless shear-rate-dependent dispersion coefficient D_{eff}/D_0 as a function of Pe^2 for a shear-thinning Carreau fluid in an axisymmetric channel for different values of Cu. Dots, crosses and circles represent the semi-analytical results, obtained by solving numerically (2.18) using (3.5) and (3.6). Purple solid, red dashed and cyan dotted lines represent the asymptotic solutions for low, intermediate and high values of Cu, respectively; see table 1. As expected, for a small Carreau number of $Cu = 0.25$, the viscosity and diffusivity depend only weakly on the shear rate and are approximately constant. As a result, the dispersion coefficient follows the Newtonian-like behaviour (purple curve) originally identified by Taylor (1953). However, as the Carreau number increases, the dispersion coefficient exceeds the Newtonian value, even at low Péclet numbers. This is due to the shear-thinning effect, which results in a decrease in viscosity and consequently enhances dispersion.

Next, we present in figure 2(*b*,*c*) the coefficients $\mathcal{A}$ and $\mathcal{B}$ as a function of Cu, which depend on the shear-thinning rheology of the Carreau fluid. We observe that both $\mathcal{A}$ and $\mathcal{B}$ monotonically increase with Cu and exceed the values of 1 and 1/48, respectively, for

https://doi.org/10.1017/jfm.2026.11682 Published online by Cambridge University Press

$Cu \geqslant 0.5$ owing to the shear-thinning effect that affects both the viscosity distribution and velocity profile. Furthermore, there is excellent agreement between the semi-analytical results and the asymptotic solutions over the wide range of values of the Carreau number. In particular, the power-law asymptotic solution (red curves) accurately captures the power-law dependence $Cu^{(1-n)/n}$ of $\mathcal{A}$ and $\mathcal{B}$ for intermediate shear rates.

3.2. *Viscoelasticity: simplified Phan-Thien–Tanner model*

To illustrate these ideas for a viscoelastic rheology, we use the simplified Phan-Thien–Tanner (sPTT) constitutive model (Phan-Thien & Tanner 1977; Phan-Thien 1978), which is derived from a Lodge–Yamamoto type of network theory and is widely used to describe the flow of concentrated polymer solutions and melts where there are strong interactions between polymer molecules. Unlike the Oldroyd-B model, which allows polymer chains, represented by elastic dumbbells, to be infinitely extensible, the sPTT model accounts for the finite extensibility of polymer chains and incorporates the shear-thinning effect, similar to the FENE-P model. At steady state, the constitutive equation for the deviatoric stress tensor $\boldsymbol{\tau}$ of the sPTT model takes the form (Phan-Thien & Tanner 1977; Phan-Thien 1978)

$$f(\boldsymbol{\tau})\boldsymbol{\tau} + \lambda[\boldsymbol{u}\cdot\boldsymbol{\nabla}\boldsymbol{\tau} - (\boldsymbol{\nabla}\boldsymbol{u})^{\mathrm{T}}\cdot\boldsymbol{\tau} - \boldsymbol{\tau}\cdot(\boldsymbol{\nabla}\boldsymbol{u})] = \mu_0(\boldsymbol{\nabla}\boldsymbol{u} + (\boldsymbol{\nabla}\boldsymbol{u})^{\mathrm{T}}) \quad \text{with} \quad f(\boldsymbol{\tau}) = 1 + \frac{\varepsilon\lambda}{\mu_0}\mathrm{tr}(\boldsymbol{\tau}). \tag{3.7}$$

In (3.7), λ is the relaxation time, μ_0 is the viscosity at zero shear rate and $f(\boldsymbol{\tau})$ is a scalar function that linearly depends on the trace of $\boldsymbol{\tau}$, where ε is the dimensionless extensibility parameter for the sPTT model. We note that another expression for $f(\boldsymbol{\tau})$ in the Phan-Thien–Tanner (PTT) model has an exponential form, $\exp(\varepsilon\lambda\mathrm{tr}(\boldsymbol{\tau})/\mu_0)$ (Phan-Thien 1978). Nevertheless, as ε is generally small, we do not expect significant differences with the results from the linear form of $f(\boldsymbol{\tau})$.

Oliveira & Pinho (1999) analysed the fully developed flow of sPTT fluid, neglecting the solvent contribution, and provided analytical expressions for the velocity, polymer stress components and viscosity distribution in an axisymmetric channel. The fully developed velocity profile of the sPTT fluid can be expressed as (Oliveira & Pinho 1999)

$$u(r) = \frac{\Delta p a^2}{4\mu_0\ell}\left(1 - \frac{r^2}{a^2}\right)\left[1 + \frac{\varepsilon\lambda^2(\Delta p)^2a^2}{4\mu_0^2\ell^2}\left(1 + \frac{r^2}{a^2}\right)\right], \tag{3.8}$$

so that the corresponding non-dimensional form of the axial velocity is

$$\tilde{u}(\tilde{r}) = 2(1-\tilde{r}^2)\left[1 + 16\varepsilon Wi^2(1+\tilde{r}^2)\right], \tag{3.9}$$

where $Wi = \lambda u_c/a$ is the Weissenberg number, which is the product of the relaxation time of the fluid, λ, and the characteristic shear rate of the flow, u_c/a. We note that $\tilde{u}'(\tilde{r})$ can be calculated from (3.9).

The corresponding dimensional and non-dimensional viscosity distributions in our notation are (Oliveira & Pinho 1999)

$$\frac{\mu(r)}{\mu_0} = \left(1 + \frac{\varepsilon\lambda^2(\Delta p)^2r^2}{2\mu_0^2\ell^2}\right)^{-1}, \qquad \mathcal{M}(\tilde{r}) = \frac{1}{1 + 32\varepsilon Wi^2\tilde{r}^2}. \tag{3.10}$$

Using (2.18) and (3.9)–(3.10), we obtain closed-form analytical expressions for the coefficients $\mathcal{A}$ and $\mathcal{B}$ in the case of the sPTT model

$$\mathcal{A} = 1 + 16\varepsilon Wi^2, \tag{3.11a}$$

https://doi.org/10.1017/jfm.2026.11682 Published online by Cambridge University Press

	Low-$\varepsilon^{1/2}Wi$ asymptote	High-$\varepsilon^{1/2}Wi$ asymptote
$\mathcal{M}(\tilde{r})$	1	$1/(32\varepsilon Wi^2\tilde{r}^2)$
$\tilde{u}(\tilde{r})$	$2(1-\tilde{r}^2)$	$32\varepsilon Wi^2(1-\tilde{r}^4)$
$\mathcal{A}$	1	$16\varepsilon Wi^2$
$\mathcal{B}$	1/48	$64\varepsilon Wi^2/135$

Table 2. A summary of the low- and high-$\varepsilon^{1/2}Wi$ asymptotic expressions for $\mathcal{M}(\tilde{r})$ and $\tilde{u}(\tilde{r})$, as well as $\mathcal{A}$ and $\mathcal{B}$ appearing in the effective shear-rate-dependent dispersion coefficient (2.18), for the case of a viscoelastic Phan-Thien–Tanner fluid in an axisymmetric channel. The results for these two distinguished limits follow in a straightforward way from (3.9)–(3.11).

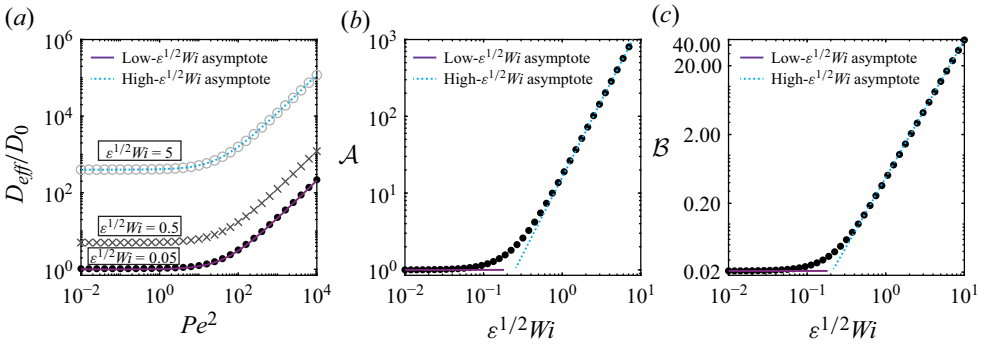


Figure 3. The effective shear-rate-dependent dispersion coefficient for a viscoelastic Phan-Thien–Tanner fluid in an axisymmetric channel. (*a*) Theoretically predicted value of D_{eff}/D_0 as a function of the square of the Péclet number, Pe^2, for different values of $\varepsilon^{1/2}Wi$. Coefficients (*b*) $\mathcal{A}$ and (*c*) $\mathcal{B}$, defined in (2.18), versus $\varepsilon^{1/2}Wi = \varepsilon^{1/2}\lambda\Delta pa/8\mu_0\ell$. Dots, crosses and circles represent the analytical results (3.11). Purple solid and cyan dotted lines represent the asymptotic solutions for $\varepsilon^{1/2}Wi \ll 1$ and $\varepsilon^{1/2}Wi \gg 1$, respectively. The asymptotic solutions are summarised in table 2.

$$\mathcal{B} = \frac{16\varepsilon Wi^2(16\varepsilon Wi^2(8\varepsilon Wi^2(195+1024\varepsilon Wi^2)+125)+75)+15}{4423680\varepsilon^3 Wi^6} - \frac{(1+48\varepsilon Wi^2+512\varepsilon^2 Wi^4)^2\ln(1+32\varepsilon Wi^2)}{9437184\varepsilon^4 Wi^8}. \tag{3.11b}$$

We have verified that as εWi^2 approaches zero, the value of $\mathcal{B}$ approaches the Newtonian limit of 1/48. We note that the non-dimensional viscosity and velocity, as well as $\mathcal{A}$ and $\mathcal{B}$, (3.11), depend solely on the single dimensionless parameter εWi^2. Therefore, we present our results as a function of $\varepsilon^{1/2}Wi$, which we refer to as the modified Weissenberg number.

We present in figure 3(*a*) the dimensionless shear-rate-dependent dispersion coefficient D_{eff}/D_0 as a function of Pe^2 for a viscoelastic Phan-Thien–Tanner fluid in an axisymmetric channel for different values of $\varepsilon^{1/2}Wi$. Dots, crosses and circles represent the analytical results (3.11). Purple solid and cyan dotted lines represent the asymptotic solutions for low and high values of $\varepsilon^{1/2}Wi$, respectively, summarised in table 2. Similar to the Carreau fluid, when $\varepsilon^{1/2}Wi$ is low (e.g. $\varepsilon^{1/2}Wi = 0.05$), the dispersion coefficient in the sPTT fluid exhibits Newtonian-like behaviour (purple curve). However, as the modified Weissenberg number increases, the dispersion coefficient surpasses the Newtonian value for all values of Péclet numbers due to enhanced shear-thinning behaviour.

https://doi.org/10.1017/jfm.2026.11682 Published online by Cambridge University Press

In addition, we show in figure 3(*b*,*c*) the coefficients $\mathcal{A}$ and $\mathcal{B}$ as a function of $\varepsilon^{1/2}Wi$, which depend on the rheology of the sPTT fluid. Similar to the behaviour of a Carreau fluid, the shear-thinning effect in the sPTT model modifies both the viscosity distribution and the velocity profile, resulting in a monotonic increase in $\mathcal{A}$ and $\mathcal{B}$ with $\varepsilon^{1/2}Wi$. We observe excellent agreement between our analytical predictions (3.11) and the asymptotic results. In particular, the high-$\varepsilon^{1/2}Wi$ asymptotic solutions provide an accurate description of both $\mathcal{A}$ and $\mathcal{B}$ even at $\varepsilon^{1/2}Wi = 1$, demonstrating their wide range of applicability.

4. Concluding remarks

In this work, we have reconsidered Taylor–Aris dispersion in pressure-driven flows of complex fluids and explicitly recognised the dependence of the diffusivity on the shear rate and the shear-rate-dependent viscosity, via an approximate Stokes–Einstein-like description; see § 2.3 for a discussion of this approximation and its limitations. In particular, based on our calculation, the general form of the dimensionless dispersion coefficient (2.18) has the expected Péclet number squared dependence, with two coefficients $\mathcal{A}$ and $\mathcal{B}$ that are dependent on the rheology of the complex fluid. Previous literature all had $\mathcal{A} = 1$ with a rheology-dependent coefficient $\mathcal{B}$, though the latter also did not incorporate a shear-rate-dependent diffusivity. We have illustrated the use of our approach by considering steady flows of a shear-thinning Carreau fluid and a viscoelastic Phan-Thien–Tanner fluid and calculating their effective shear-rate-dependent axial dispersion coefficients.

Finally, we note that Taylor–Aris dispersion analysis in pressure-driven flows of shear-rate-dependent fluids may be further complicated when one accounts for the non-isotropic nature of the fluid properties. To recognise some of the complexities that arise for the general problem, consider the case in this work of steady channel flows that involve viscosity variations with shear rate, i.e. the viscosity is a scalar field of position. However, the corresponding diffusivity may take the form of a second-order tensor field, since the resistance to a motion of a sphere (or the force–velocity relation) will be different for motions along as compared with transverse to the viscosity gradient. This detail would then enter the advection–diffusion (2.1) and subsequent steps. For example, the components D_{rr} and D_{zz}, respectively, would enter the radial and axial diffusive terms, which, in the simplest case, would influence results as $\mathcal{A}$ would then involve D_{zz} and $\mathcal{B}$ would involve D_{rr}. Clearly, there are significant theoretical questions to think about to better characterise dispersion in the flows of complex fluids.

Acknowledgements. We thank J. C. Conrad for a helpful discussion on colloidal diffusion in polymer solutions.

Funding. E.B. acknowledges the support by grant no. 2022688 from the US-Israel Binational Science Foundation (BSF) and the Israeli Council for Higher Education Yigal Alon Fellowship. H.A.S. acknowledges the support from grant no. CBET-2246791 from the United States National Science Foundation (NSF).

Declaration of interests. The authors report no conflict of interest.

References

Aris, R. 1956 On the dispersion of a solute in a fluid flowing through a tube. *Proc. R. Soc. Lond. A* **235** (1200), 67–77.

Bird, R.B., Armstrong, R.C. & Hassager, O. 1987 *Dynamics of Polymeric Liquids. Volume 1: Fluid Mechanics*, 2nd edn. John Wiley and Sons.

Booras, G.S. & Krantz, W.B. 1976 Dispersion in the laminar flow of power-law fluids through straight tubes. *Ind. Engng Chem. Fundam.* **15** (4), 249–254.

https://doi.org/10.1017/jfm.2026.11682 Published online by Cambridge University Press

BOYKO, E. & STONE, H.A. 2021 Flow rate–pressure drop relation for shear-thinning fluids in narrow channels: approximate solutions and comparison with experiments. *J. Fluid Mech.* **923**, R5.

BROCHARD-WYART, F. & DE GENNES, P.G. 2000 Viscosity at small scales in polymer melts. *Eur. Phys. J. E* **1** (1), 93–97.

CAI, L.-H., PANYUKOV, S. & RUBINSTEIN, M. 2011 Mobility of nonsticky nanoparticles in polymer liquids. *Macromolecules* **44** (19), 7853–7863.

CARREAU, P.J. 1972 Rheological equations from molecular network theories. *Trans. Soc. Rheol.* **16** (1), 99–127.

CHEN, R.P.-S., NIKOUBASHMAN, R., HOWARD, A., M., P., CONRAD, J.C. & PALMER, J.C. 2018 Coupling of nanoparticle dynamics to polymer center-of-mass motion in semidilute polymer solutions. *Macromolecules* **51** (5), 1865–1872.

DASH, R.K., JAYARAMAN, G. & MEHTA, K.N. 2000 Shear augmented dispersion of a solute in a Casson fluid flowing in a conduit. *Ann. Biomed. Engng* **28** (4), 373–385.

DATT, C. & ELFRING, G.J. 2019 Active particles in viscosity gradients. *Phys. Rev. Lett.* **123**, 158006.

ESPARZA LÓPEZ, C., GONZALEZ-GUTIERREZ, J., SOLORIO-ORDAZ, F., LAUGA, E. & ZENIT, R. 2021 Dynamics of a helical swimmer crossing viscosity gradients. *Phys. Rev. Fluids* **6** (8), 083102.

FAN, L.T. & HWANG, W.S. 1965 Dispersion of Ostwald–de Waele fluid in laminar flow through a cylindrical tube. *Proc. R. Soc. Lond. A* **283** (1395), 576–582.

FURST, E.M. & SQUIRES, T.M. 2017 *Microrheology*. Oxford University Press.

GRIFFITHS, I.M. & STONE, H.A. 2012 Axial dispersion via shear-enhanced diffusion in colloidal suspensions. *Europhys. Lett.* **97** (5), 58005.

KOHLI, I. & MUKHOPADHYAY, A. 2012 Diffusion of nanoparticles in semidilute polymer solutions: effect of different length scales. *Macromolecules* **45** (15), 6143–6149.

LIEBCHEN, B., MONDERKAMP, P., TEN HAGEN, B. & LÖWEN, H. 2018 Viscotaxis: microswimmer navigation in viscosity gradients. *Phys. Rev. Lett.* **120** (20), 208002.

MAHAPATRA, B., RUANGKRIENGSIN, T., STONE, H.A. & BOYKO, E. 2025 Viscoelastic fluid flow in a slowly varying planar contraction: the role of finite extensibility on the pressure drop. *J. Fluid Mech.* **1009**, A12.

MALGARETTI, P., POPESCU, M.N. & DIETRICH, S. 2016 Active colloids at fluid interfaces. *Soft Matt.* **12** (17), 4007–4023.

NAGARANI, P. & SEBASTIAN, B.T. 2013 Dispersion of a solute in pulsatile non-Newtonian fluid flow through a tube. *Acta Mechanica* **224** (3), 571–585.

NATH, P., MANGAL, R.K., CHOUDHURY, F., NARAYANAN, S., WIESNER, S., U, & ARCHER, L.A. 2018 Dynamics of nanoparticles in entangled polymer solutions. *Langmuir* **34** (1), 241–249.

OLIVEIRA, P.J. & PINHO, F.T. 1999 Analytical solution for fully developed channel and pipe flow of Phan-Thien–Tanner fluids. *J. Fluid Mech.* **387**, 271–280.

OPPENHEIMER, N., NAVARDI, S. & STONE, H.A. 2016 Motion of a hot particle in viscous fluids. *Phys. Rev. Fluids* **1** (1), 014001.

PHAN-THIEN, N. 1978 A nonlinear network viscoelastic model. *J. Rheol.* **22** (3), 259–283.

PHAN-THIEN, N. & TANNER, R.I. 1977 A new constitutive equation derived from network theory. *J. Non-Newtonian Fluid Mech.* **2** (4), 353–365.

RANA, J. & MURTHY, P.V.S.N. 2016*a* Solute dispersion in pulsatile Casson fluid flow in a tube with wall absorption. *J. Fluid Mech.* **793**, 877–914.

RANA, J. & MURTHY, P.V.S.N. 2016*b* Unsteady solute dispersion in non-Newtonian fluid flow in a tube with wall absorption. *Proc. R. Soc. Lond. A* **472** (2193), 20160294.

RINGS, D., SCHACHOFF, R., SELMKE, M., CICHOS, F. & KROY, K. 2010 Hot Brownian motion. *Phys. Rev. Lett.* **105** (9), 090604.

SHARP, M.K. 1993 Shear-augmented dispersion in non-Newtonian fluids. *Ann. Biomed. Engng* **21** (4), 407–415.

SINGH, S. & MURTHY, P.V.S.N. 2023 Significance of skewness and kurtosis on the solute dispersion in pulsatile Carreau–Yasuda fluid flow in a tube with wall absorption. *J. Fluid Mech.* **962**, A42.

SQUIRES, T.M. & MASON, T.G. 2010 Fluid mechanics of microrheology. *Annu. Rev. Fluid Mech.* **42** (1), 413–438.

STONE, H.A. & BRENNER, H. 1999 Dispersion in flows with streamwise variations of mean velocity: radial flow. *Ind. Engng Chem. Res.* **38** (3), 851–854.

TAYLOR, G.I. 1953 Dispersion of soluble matter in solvent flowing slowly through a tube. *Proc. R. Soc. Lond. A* **219** (1137), 186–203.

TEODORO, C., BAUTISTA, O. & MÉNDEZ, F. 2025 Taylor dispersion analysis in a viscoelastic fluid through arbitrarily shaped axisymmetric channels. *J. Fluid Mech.* **1025**, A9.

ZHONG, X., MITRA, H., VEILLEUX, J.-C., SIMMONS, E., SHI, G.H. & ARDEKANI, A.M. 2022 The role of liquid rheological properties on the injection process of a spring-driven autoinjector. *Intl J. Pharm.* **628**, 122296.

https://doi.org/10.1017/jfm.2026.11682 Published online by Cambridge University Press